doi: 10.1111/j.1751-3928.2008.00054.x *Resource Geology* Vol. 58, No. 2: 143–160

Original Article

Geology and Re-Os Geochronology of Mineralization of the Miduk Porphyry Copper Deposit, Iran

Nader Taghipour[1], Alijan Aftabi[1] and Ryan Mathur[2]

[1]*Department of Geology, Shahid Bahonar University of Kerman, Kerman, Iran* [2]*Department of Geology, Juniata College, Huntingdon, Pennsylvania, USA*

Abstract

The Miduk porphyry copper deposit is located in Kerman province, 85 km northwest of the Sar Cheshmeh porphyry copper deposit, Iran. The deposit is hosted by Eocene volcanic rocks of andesitic–basaltic composition. The porphyry-type mineralization is associated with two Miocene calc-alkaline intrusive phases (P1 and P2, respectively). Five hypogene alteration zones are distinguished at the Miduk deposit, including magnetite-rich potassic, potassic, potassic–phyllic, phyllic and propylitic. Mineralization occurs as stockwork, dissemination and nine generations (magnetite, quartz–magnetite, barren quartz, quartz-magnetite-chalcopyrite-anhydrite, chalcopyrite–anhydrite, quartz-chalcopyrite-anhydrite-pyrite, quartz-molybdenite-anhydrite ± chalcopyrite ± magnetite, pyrite, and quartz-pyrite-anhydrite ± sericite) of veinlets and veins. Early stages of mineralization consist of magnetite rich veins in the deepest part of the deposit and the main stage of mineralization contains chalcopyrite, magnetite and anhydrite in the potassic zone. The high intensity of mineralization is associated with P2 porphyry (Miduk porphyry). Based on petrography, mineralogy, alteration halos and geochemistry, the Miduk porphyry copper deposit is similar to those of continental arc setting porphyry copper deposits. The Re-Os molybdenite dates provide the timing of sulfide mineralization at 12.23 ± 0.07 Ma, coincident with U/Pb zircon ages of the P2 porphyry. This evidence indicates a direct genetic relationship between the Miduk porphyry stock and molybdenite mineralization. The Re-Os age of the Miduk deposit marks the main stage of magmatism and porphyry copper formation in the Central Iranian volcano-plutonic belt.

Keywords: alteration, central Iranian volcano-plutonic copper belt, Miduk porphyry copper deposit, mineralization, Re-Os geochronology.

1. Introduction

The southeast segment of the Central Iranian volcano-plutonic belt (Kerman belt) in the Kerman Province is one of the major copper-producing regions in the Alps–Himalaya orogen (Fig. 1). The extensive volcanism, plutonism and mineralization are related to subduction of the Neotethys lithosphere beneath Central Iran along the Zagros reverse fault (Forster, 1978; Berberian & King, 1981; Hassanzadeh, 1993; Aftabi & Atapour, 2000). Porphyry copper mineralization occurs in close proximity to granitoid intrusive rocks of Miocene age in the Central Iranian volcano-plutonic belt (CIVPB; Fig. 1). In addition to CIVPB, two major tectonic elements including the Sanandaj–Sirjan metamorphic zone and the Zagros fold–thrust belt are recognized in western and southwestern Iran (Alavi, 1994; Mohajjel *et al*., 2003). More than 50 porphyry-vein type deposits occur in this belt. The length of the Kerman volcano-plutonic belt is approximately 450 km with an average width of

Received 6 May 2007. Accepted for publication 29 August 2007.
Corresponding author: N. TAGHIPOUR, Department of Geology, Shahid Bahonar University of Kerman, Kerman 76135, Iran.
Email: n.taghipour@graduate.uk.ac.ir

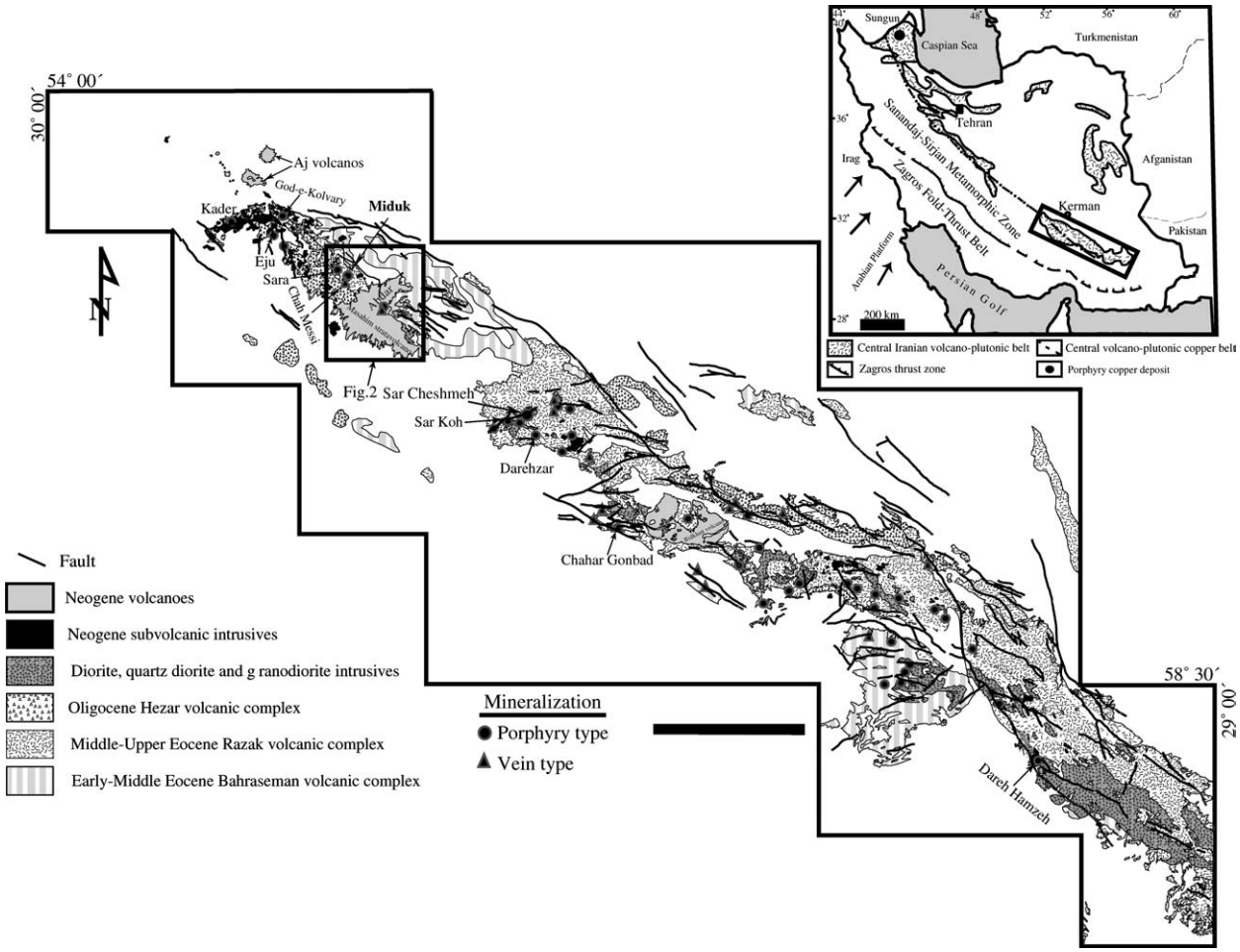

Fig. 1 Central Iranian volcano-plutonic copper belt and study area in the Kerman Belt (modified after Institute for Geological and Mining Exploration and Institution of Nuclear and Other Mineral Raw Materials, 1973). Bar, 50 km.

80 km. The Sar Cheshmeh porphyry copper deposit is the largest deposit in the area with 1200 Mt of ore at 0.69% Cu and 0.03% Mo (Shahabpour, 2000).

The Miduk porphyry copper deposit is located in the Shahr-Babak area in Kerman province, Iran. This deposit is located 85 km NW of the Sar Cheshmeh porphyry copper deposit (Fig. 1). Preliminary mineral exploration in this area was carried out in 1967–1970 by Parjam and Metallgesellschaft (Hassanzadeh, 1993). So far, more than 50 diamond drill holes with a maximum depth of 1013 m have proved the existence of the sizeable and potential porphyry copper mineralization at the Miduk deposit. The orebody contains 170 million tons of ore, with an average grade of 0.86% Cu, 0.007% Mo, 82 ppb Au and 1.8 ppm Ag. Supergene enrichment blankets average approximately 50 m thickness and comprise the primary source of Cu ore.

To further understand the regional and local geologic relationships and timing of mineralization, this contribution presents aspects of petrography, alteration, mineralization, vein classification and Re-Os isotope age of molybdenite in the Miduk deposit.

2. Regional geology of Miduk area

The oldest units in the area (Fig. 2) are Cenomanian–Turonian calcareous flysch (Saric *et al.*, 1971) that are unconformably overlain by Paleocene Kerman conglomerate (Dimitrijevic, 1973) and subsequently covered by Eocene flysch (Saric *et al.*, 1971; Dimitrijevic, 1973). All of these units are in turn covered by Paleogene volcanic complexes.

Three volcanic complexes cross-cut these Cretaceous–Paleocene rocks in the Miduk area (Fig. 2).

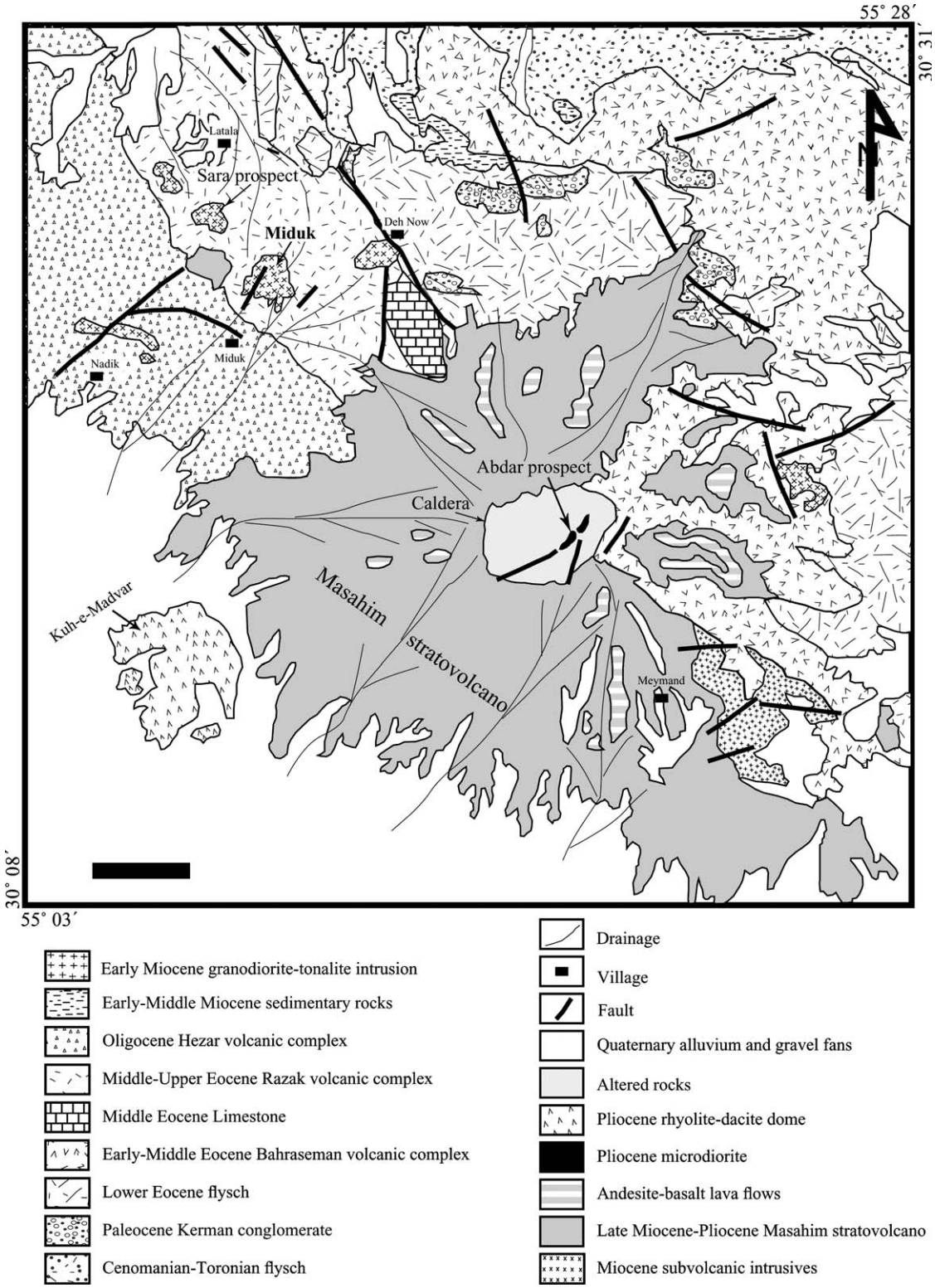

Fig. 2 Regional geological map of the Miduk area (modified after Saric *et al.*, 1971; Dimitrijevic, 1973). Bar, 5 km.

The oldest, Bahraseman volcanic complex formed in the Lower Eocene and began with an explosive phase of acidic pyroclastics, tuffs and volcanic breccias, separated mainly by rhyolite flows (Dimitrijevic, 1973). This complex is the earliest volcanic activity of Tertiary age in the southern part of the Iranian volcano-plutonic belt in Kerman province. The thickness of this complex is estimated to be approximately 7 km, but in the Miduk area it is approximately 400–500 m. Razak volcanic complex is the main host rock to the Miduk porphyry copper deposit and is subdivided into three units: a lower mainly basic subcomplex (trachybasalt, andesite and trachyandesite); a middle, acidic subcomplex (acidic tuff); and an upper, basic subcomplex (trachyandesite and andesite-basalt) (Dimitrijevic, 1973).

$^{40}Ar/^{39}Ar$ dating of albite from the lower unit of this complex yielded an age of 37.5 ± 1.4 Ma for the volcanic rocks (Hassanzadeh, 1993). The youngest volcanic complex of Paleogene, Hezar, consists of appreciable amounts of acidic rocks. This complex covers large parts of the Miduk area and mainly consists of trachyandesite and trachybasalt. $^{40}Ar/^{39}Ar$ dating of analcime of this complex yielded an age of 32.7 ± 6.3 Ma (Hassanzadeh, 1993) for the Hezar complex.

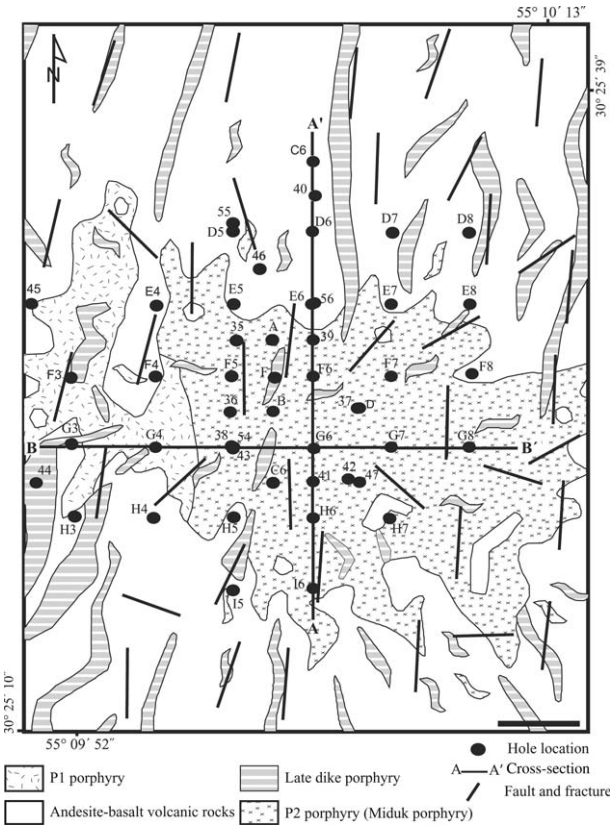

Fig. 3 Geological map of the Miduk porphyry copper deposit (modified after Outomec, 1992) (•) Drill hole locations.

Younger porphyry intrusions in the Miduk area include three phases, ranging from Miocene to Pliocene age. Miocene plutonic bodies intruded the aforementioned Paleogene volcanogenic complexes. Based on structural level of exposure, they can be subdivided into two distinct groups (Dimitrijevic, 1973; Hassanzadeh, 1993). The first group is represented by a shallowly emplaced stock of granodiorite–tonalite that is partly covered by the late Miocene–Pliocene volcanic and subvolcanic rocks and located southeast of the Masahim (Abdar) stratovolcano (Fig. 2). The other groups of the Miocene intrusions occur as smaller bodies that represent even shallower parts of the subvolcanic system. These are diorite and quartz–diorite porphyries, principally containing andesine, hornblende and biotite phenocrysts in a groundmass of plagioclase, quartz and K-feldspar. Porphyry copper mineralization at Miduk is associated with the shallow intrusive rocks (Fig. 3).

The youngest intrusions in this area are subvolcanic rocks formed in a caldera of Masahim (Abdar) that generated the Abdar Pb-Cu mineralization. $^{40}Ar/^{39}Ar$ age dating of biotite and hornblende of the lava flows and flanks of Masahim (Abdar) stratovolcano and U/Pb dating of zircon intrusion yielded 6.8 ± 0.4 Ma, 6.4 ± 0.8–6.3 ± 0.9 Ma, and 7.5 ± 0.1 Ma, respectively (Hassanzadeh, 1993; McInnes *et al.*, 2005). The youngest subvolcanic and volcanic phases that mainly occurred in the Miduk area began in the Pliocene and consist of dacitic domes and lava plugs and Masahim stratovolcano (Fig. 2).

3. Methods

For the study of petrography, alteration and mineralization and vein classification, many samples were collected from drill holes and outcrops. The location of the samples is shown in Figures 4, 5. A total of 45 thin sections, 43 polished thin sections and 54 polished sections were prepared. The modal mineralogy for petrographical study was calculated according to volume % estimation diagrams (Hutchinson, 1974).

For the Re-Os dating of molybdenite, we handpicked flakes of molybdenite from veins. We dissolved the samples using the carius tube method (Shirey & Walker, 1995), and distilled the solution for extraction of Re and Os (Frei *et al.*, 1998; Mathur, 2000). Concentrations were determined by isotope dilution, and we used two non-mixed spikes, ^{185}Re-enriched spike

(161.58 ppm) and ^{190}Os-enriched spike (99.84 ppb) for molybdenite. Samples were measured on a negative thermal ionization mass spectrometer at Arizona University, using loading and instrument procedures that are described in Creaser *et al.* (1991).

Molybdenite ages are calculated by assuming no initial ^{187}Os, similar to McCandless and Ruiz (1993). The decay constant used for ^{187}Re was 1.666×10^{-11} year^{-1} ± 1% (Smoliar *et al.*, 1996). Errors are calculated based on the calibration of the spike (0.22–0.4%), and the uncertainty of the decay constant of Re. Repeat analyses indicate an error on analysis of ± 0.5% for each element.

4. Mine geology

The extrusive rocks are exposed in the mine area and are host rock for mineralization; although they are described as basaltic andesite and andesite (Hassanzadeh, 1993), they are andesitic basalt. These rocks are usually massive, with textures that range from aphanitic, through to fine-grained and porphyritic. The porphyritic rocks are composed of 60 vol% plagioclase phenocrysts and the matrix contained plagioclase, pyroxene, sericite and magnetite and pyrite that replace ferromagnesian minerals and glass. The mineralized intrusive rocks at

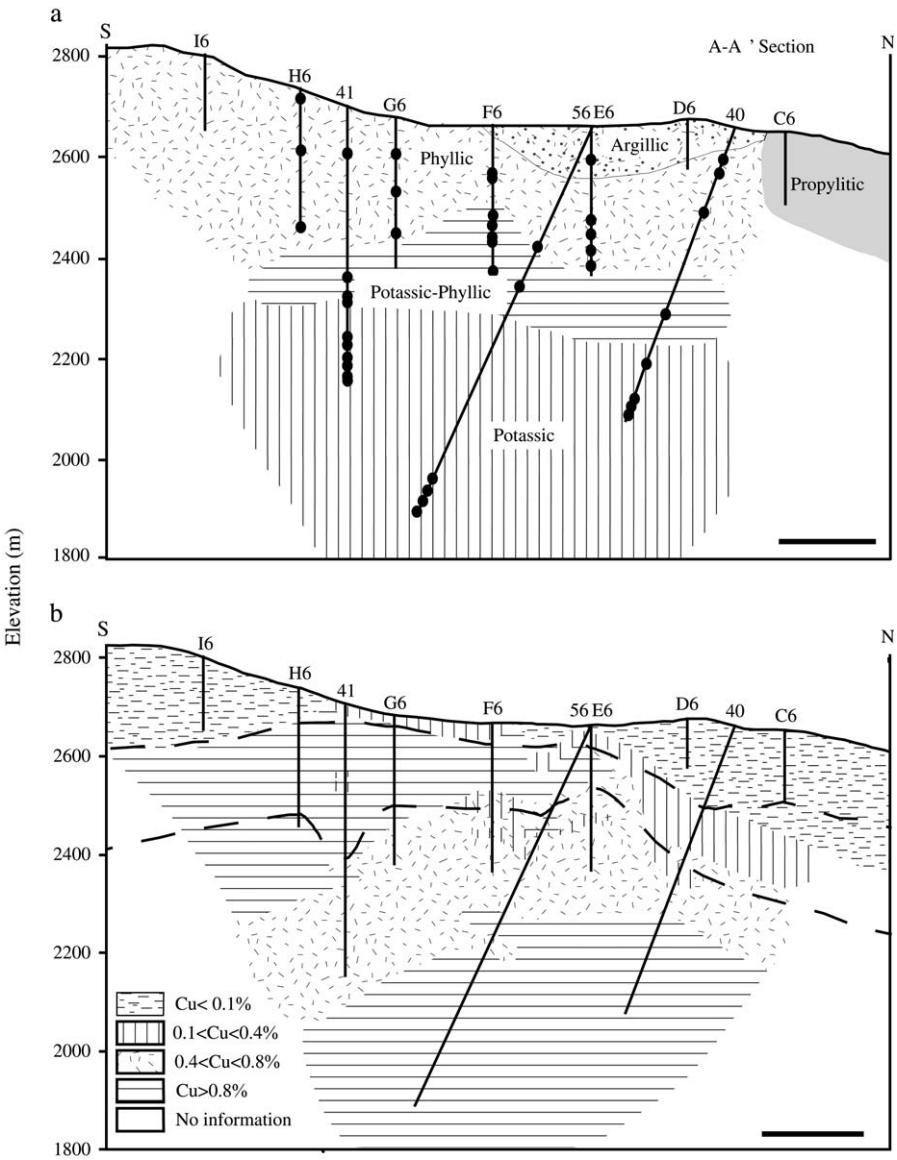

Fig. 4 Distribution of (a) alteration patterns and (b) Cu grades along cross-section A-A′ in Figure 3. Numbers on the surface indicate drill holes; (•) location of the samples for petrography and vein classification studies; (– –) base of the oxide and supergene zone. Bars, 100 m.

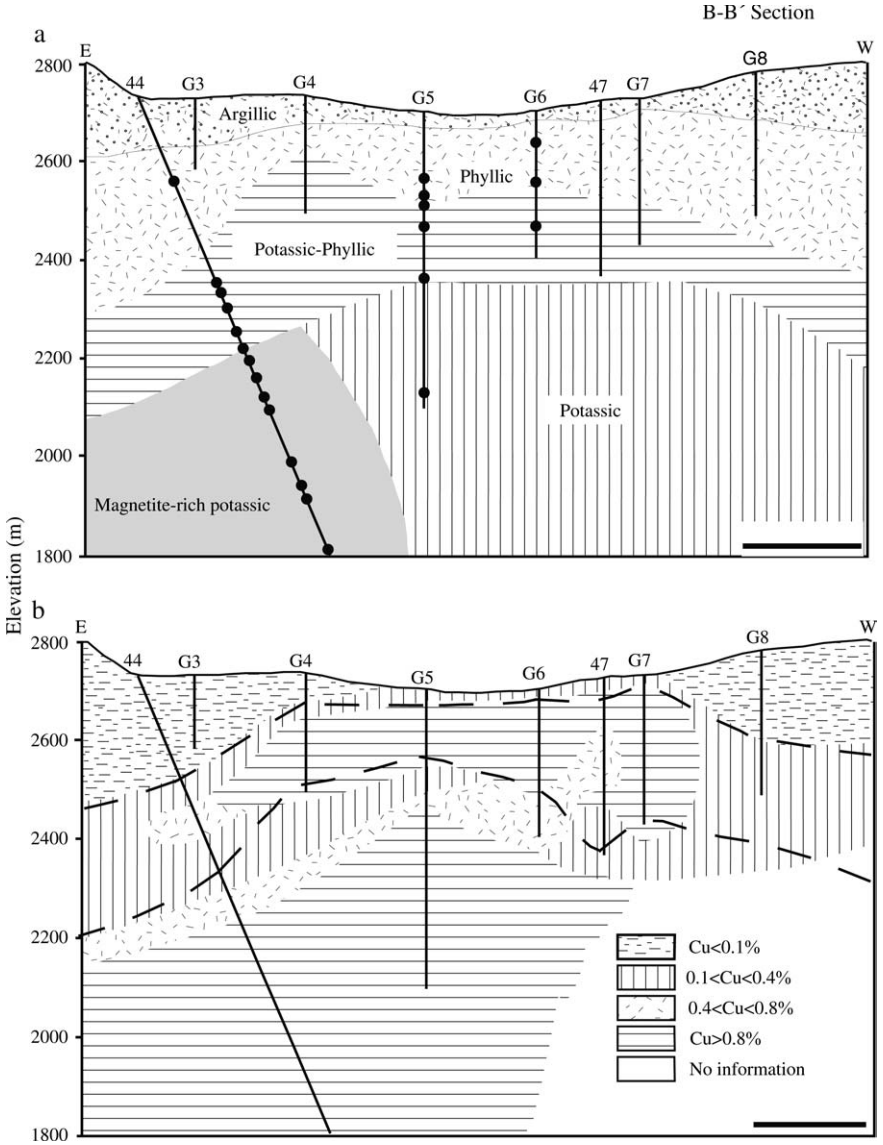

Fig. 5 Distribution of (a) alteration patterns and (b) Cu grades along cross-section B-B′ in Figure 3 with neighboring holes 50 m south from this section. Numbers on the surface indicate drill holes; (•) location of the samples for petrography and vein classification studies; (– –) base of the oxide and supergene zone. Bars, 100 m.

the Miduk deposit cover an area of approximately 0.7 km × 1 km and at least three major temporal stages of intrusive phases can be distinguished on the basis of texture, cross-cutting relations and intensity of mineralization (Fig. 3): (i) P1 porphyry; (ii) P2 diorite–quartz diorite porphyry (Miduk porphyry); and (iii) and late dike porphyry.

Structurally, any major faults have not been found in the open pit of the Miduk deposit. The dominant fractures in the Miduk deposit are NS, EW and radial. Vertical NS-orientated fractures are visible on a large area around the Miduk deposit. The intensity of these NS-fracturing systems can be seen in late porphyry dikes, which were not mineralized. The P1 porphyry present only in the western part of the Miduk deposit (Fig. 3). It has a porphyry–aplitic texture and is gray and strongly altered. Currently, no fresh part has been found. Well-developed, extensive veining occurs with magnetite mineralization as stockwork, disseminations and fracture fillings. The alteration in P1 porphyry is not as extensive as P2 porphyry. The P2 diorite–quartz diorite porphyry (Miduk porphyry) is the largest intrusive phase at the Miduk deposit and covers most of the deposit at the current surface. It is strongly altered, mineralized and characterized by preserved plagioclase phenocrysts, biotite and quartz. This intrusion is strongly stockworked,

veined, mineralized and altered to quartz, K-feldspar and secondary biotite. Both P1 and P2 porphyries and the andesite–basalt volcanic rocks have been intersected by numerous late porphyry dikes with a NS trend (Fig. 3). Petrographically, these dikes are related to diorite–quartz diorite porphyry and are easily distinguishable from other porphyries by weak alteration and mineralization.

Quaternary shallowly emplaced olivine–basalt dikes without any link to porphyry mineralization are also present in the Miduk area (Hassanzadeh, 1993).

5. Petrography of intrusive phases at the Miduk deposit

Petrographic observations of polished thin sections indicate that P1 porphyry is highly altered and contains 40–50 vol% of phenocrysts consisting mainly of plagioclase, quartz, biotite and hornblende. The primary composition of plagioclases is unclear and all of them have been altered, as well as hornblende and biotite phenocrysts. The groundmass of this intrusive phase consists mainly of fine-grained quartz, biotite, plagioclase, K-feldspar and anhydrite.

The P2 porphyry contains 50 vol% plagioclase phenocrysts, 13–15 vol% quartz and approximately 10 vol% biotite. Plagioclase phenocrysts of the intrusion are calcic, euhedral and are somewhat altered to sericite.

Amphibole phenocrysts are completely altered to secondary biotite and magnetite. Accessory minerals include apatite, zircon, magnetite, rutile, and titanite, which occur as inclusions in the silicate phases and interstices between them.

The late dike porphyry is characterized by abundant plagioclase phenocrysts, relatively minor quartz and hornblende phenocrysts and euhedral and fresh phenocrysts of biotite. These phenocrysts contain more than 60 vol% of this dike. Hornblende is altered to chlorite and magnetite. Fine-grained quartz, plagioclase and apatite compose the groundmass of this dike.

Table 1 details petrographic characteristics of intrusive rocks at the Miduk porphyry copper deposit.

6. Alteration and mineralization

Alteration at the Miduk deposit was studied by the Institute for Geological and Mining Exploration and Institution of Nuclear and Other Mineral Raw Materials (1973) and Hassanzadeh (1993). Hassanzadeh (1993) distinguished five stages of alteration (potassic, sodic–potassic, sodic, phyllic and propylitic). The present evidence indicates alteration and mineralization at six stages, which are described from oldest to youngest. Hydrothermal alteration and mineralization were mainly focused on the P1 and P2 porphyries (Figs. 4, 5).

6.1. Magnetite-rich potassic alteration

An early stage alteration as distinguished in the present study generated a magnetite-rich zone in the P1 porphyry and volcanic wall rocks, in which magnetite mineralization occurred as veinlets (M1 type) and veins (M2 type) and dissemination (Table 2). This alteration is characterized by magnetite, quartz, K-feldspar and a minor amount of secondary biotite and sericite. Chalcopyrite is the main Cu-bearing mineral in this alteration and occurs as dissemination and vein mineralization (2–10 mm). This alteration is superimposed by sericite-clay-chlorite alteration.

6.2. Potassic alteration

Two different potassic alteration zones according to mineral assemblages were distinguished. First, weakly altered rocks are characterized by fresh and euhedral plagioclase with secondary biotite occurring in the matrix and replacing hornblende and a smaller amount of magmatic biotite. This alteration is present in the deepest and central part of the deposit. Second, strong potassic alteration is characterized by secondary K-feldspar in the plagioclase rims and in the matrix, shreddy biotite that completely replaces ferromagnesian minerals, and anhydrite. The extensive distribution of secondary biotite is observed in andesite–basalt rocks. Magnetite mineralization in this zone is common as dissemination and vein with quartz + chalcopyrite + anhydrite. Chalcopyrite is the main Cu mineral and occurs as dissemination, intergrowth with magnetite, vein with quartz-anhydrite-magnetite and as veinlets with anhydrite. Pyrite veinlets also are present in this alteration. Scarce amount of bornite is present with chalcopyrite in this zone. Barren quartz veinlets/veins occur in this alteration and cut plagioclase phenocrysts and primary biotites.

6.3. Propylitic alteration

This alteration occurs in the peripheral zone of the P2 porphyry body and especially in the northern part of the deposit. The propylitic alteration was not observed in the deeper part and in the transitional zone with potassic alteration. It also occurs in volcanic rocks in which mafic minerals are altered to chlorite, epidote,

Table 1 Petrographic characteristics of different rock types at the Miduk porphyry copper deposit

Rock type	Mineral content (vol%)	Matrix	Vein density (%)	Alteration zone	Intensity of Cu mineralization
Andesite–basalt	Plagioclase: 60; Pyroxene: 10–15; Olivine: 3; Matrix: 25	Fine to medium-grained, plagioclase, pyroxene, sericite and ore minerals	1–5	Phyllic, propylitic	Weak
P1 porphyry	Plagioclase: 15–20; Quartz: 20; Biotite: 10; Matrix: 50	Highly altered, fine-grained, quartz, biotite, plagioclase, K-feldspar, anhydrite	30	Magnetite-rich potassic, potassic-phyllic and phyllic	Moderate to strong
P2 porphyry (Miduk porphyry)	Plagioclase: 50; Quartz: 10–15; Hornblende: 5; Biotite:10; Matrix: 25	Coarse-grained, quartz, biotite, plagioclase, K-feldspar, anhydrite	10–>60	Intensely potassic, potassic-phyllic and phyllic	Strong
Late dike porphyry	Plagioclase: 40; Hornblende: 15; Biotite: 5; Matrix: 40	Fine-grained, quartz, plagioclase, apatite	<1	Commonly unaltered	Weak
Olivine-basalt dike	Pyroxene: 15–20; Olivine:30; Matrix: 50	Very fine-grained, plagioclase pyroxene, olivine, biotite	—	Commonly unaltered	Barren

calcite and pyrite. Plagioclase phenocrysts are altered to sericite, chlorite and epidote.

6.4. Potassic–phyllic alteration

This alteration is relatively widespread (Figs 4a, 5a) and was formed by overlapping of phyllic assemblage on potassic alteration. In this zone, plagioclase is completely altered to K-feldspar, sericite and clay minerals ± anhydrite; and biotite is altered to secondary biotite–sericite and rutile aggregates. Pyrite and chalcopyrite are the most common sulfide minerals that occur as vein and dissemination. Magnetite displays dissemination and vein with quartz-chalcopyrite-pyrite-anhydrite.

6.5. Phyllic alteration

Phyllic or sericitic alteration is formed by the leaching of sodium, calcium and magnesium from aluminosilicate-bearing rocks. It is distinguished by the presence of quartz, sericite and pyrite. Almost all of the rock-forming minerals are completely altered to sericite, pyrite and quartz. Anhydrite and titanite are accessory minerals in this zone. The change from potassic–phyllic alteration to phyllic alteration is gradual and is characterized by the increase in amounts of sericite and quartz. Pyrite is the most important mineral in the veins and also occurs as dissemination in this zone.

6.6. Argillic alteration

This alteration is not particularly common as primary hydrothermal effects, but occurs instead most typically as a result of supergene processes (e.g. Beane & Bodnar, 1995). All rock-forming minerals are completely altered to clay minerals, sericite, quartz and hematite. This alteration occurs in the upper part of the Miduk deposit. Based on X-ray diffraction, kaolinite is the dominant phyllosilicate and is accompanied by illite.

7. Vein classifications

The stockwork system at the Miduk porphyry copper deposit is developed mainly in the central and deeper parts of the deposit. On the basis of petrography, mineralogical data and cross-cutting relationships, nine different types of veins were distinguished (Table 2). Paragenetic sequences of these veins are shown in Table 3.

Table 2 Vein classification at the Miduk porphyry copper deposit

Vein type	Mineralogy	Alteration mineralogy	Shape and size	Crosscutting relationships and occurrences	Alteration zone	Alphabetic classification
I	Magnetite	None to K-feldspar	Irregular thin veinlets (<1–2 mm)	Cut plagioclase phenocrysts, Present in P2	Magnetite-rich potassic	M_1
II	Quartz-magnetite ± chalcopyrite	K-feldspar and magnetite	continuous, 2–15 mm wide	Cut magnetite veinlets, present mainly in P2 porphyry	Magnetite-rich potassic	M_2
III	Quartz-anhydrite in central part white lines of calcite, K-feldspar and sericite	None at veinlets, K-feldspar	Continuous and varied in wide (1–20 mm)	Cuts plagioclase and primary biotite, quartz-magnetite veins and cut by later chalcopyrite veins and occur in P1 and P2	Potassic	B_1
IV	Quartz-magnetite-chalcopyrite-anhydrite ± K-feldspar ± pyrite	K-feldspar, biotite	Continuous, 5–20 mm wide	Cut I and II vein types and occur in P1 and P2	Potassic, potassic-phyllic, phyllic	A_1
V	Chalcopyrite-anhydrite	K-feldspar	Thin (1–2 mm), continuous	Cuts plagioclase phenocrysts, barren quartz and quartz-magnetite veins	Potassic	A_2
VI	Quartz-chalcopyrite-anhydrite-pyrite	K-feldspar, biotite, sericite	Continuous and thicker than V type, sulfides are located in center line of vein	Cuts barren quartz veins and cut by pyrite veins Present in P1 and P2 porphyry	Potassic, potassic-phyllic, phyllic	C
VII	Quartz-molybdenite ± magnetite ± chalcopyrite ± anhydrite	K-feldspar, minor sericite	Irregular thin (<5 mm)	No crosscutting relationship is distinguished with other vein types, occur mainly in P2	Potassic	B_2
VIII	Pyrite ± quartz	K-feldspar, quartz, sericite	Relatively narrow (<1 mm) and planar	Cuts III and VI vein types	Phyllic, potassic	D_1
IX	Quartz-pyrite-anhydrite ± sericite	Quartz, sericite	Continuous and thickest veins (10–50 mm). pyrite is located in center of vein	Commonly is present in andesite-basalt wall rocks and in P1 and P2 porphyries.	Phyllic	D_2

7.1. Magnetite veinlets

These veinlets were formed during the initial fracturing of the porphyry and mainly consist of magnetite. They are thin, discontinuous and <2 mm wide. Magnetite grains are anhedral to subhedral. These veinlets are present only in deeper parts of P1 porphyry (Fig. 6a). Sulfides are absent in these veinlets. Based on the structural irregularities, the magnetite veinlets formed at a relatively high temperature, when the P1 porphyry was relatively ductile. They were formed in the early stage of mineralization. Magnetite veinlets (type I) and quartz–magnetite veins (type II) are especially associated with magnetite-rich potassic alteration zone.

7.2. Quartz–magnetite veins

These veins are more regular, continuous and thicker than type I and occur within magnetite-rich potassic alteration zone. The thickness ranges from 3 to 15 mm (Fig. 6b, c). They consist of granular and euhedral quartz and anhedral magnetite. Chalcopyrite is present in a minor amount. These veins have been observed in the P1 porphyry. The thickness of the veins increases with decreasing depth. The ratio of quartz to magnetite varies and magnetite mainly exists in the central part of the veins. These veins generally cut magnetite veinlets (Fig. 6b). K-feldspar and disseminated magnetite are alteration minerals that envelop these veins.

7.3. Barren quartz veins

They are relatively narrow and consist predominantly of quartz and anhydrite with minor chalcopyrite. Quartz crystals have a mosaic to granular texture and are coarser than those in the matrix. Anhydrite crystals are granular and have the same size as quartz. K-feldspar is the main alteration mineral around these veins (Fig. 6d) and occurs in the P2 porphyry and potassic alteration zone. Where these veins cut through plagioclase phenocrysts and primary biotite, a thin halo of feldspar and secondary biotite is developed along the vein walls. The formation of orthoclase and secondary biotite around these veins, cross-cutting plagioclase and primary biotite, shows that they were developed during the early stage of potassic alteration. Some of these veins contain calcite, feldspar and sericite in the center of the veins (Fig. 6e), and are cut by pyrite veins (Fig. 6f).

7.4. Quartz-magnetite-chalcopyrite-anhydrite veins

These veins are continuous and regular and consist mainly of magnetite and chalcopyrite (Fig. 6b). The size of these veins varies from 5 to 20 mm. The central zone of the vein is composed of chalcopyrite, magnetite, calcite and sericite. The sizes of the chalcopyrite and magnetite grains are 1–20 μm and 1–30 μm, respectively. Pyrite is an accessory mineral with a diameter of 10–30 μm. In some of these veins, magnetite is located in the margin of the veins. K-feldspar and secondary

Table 3 Schematic paragenetic sequences of veins in Miduk porphyry copper deposit

Vein type	Vein mineralogy	Early mineralization	Main mineralization	Late mineralization
I	Mag			
II	Qz+Mag±Cpy			
III	Qz+Anhy			
IV	Qz+Mag+Cpy+Anhy±K-feld±Py			
V	Cpy+Anhy			
VI	Qz+Cpy+Anhy+Py			
VII	Qz+Mo±Cpy±Mag±Anhy			
VIII	Py±Qz			
IX	Qz+Py+Anhy±Ser			

Anhy: anhydrite, Cpy: chalcopyrite, K-feld: K-feldspar, Mag: magnetite, Mo: molybdenite, Py: pyrite, Qz: quartz, Ser: sericite

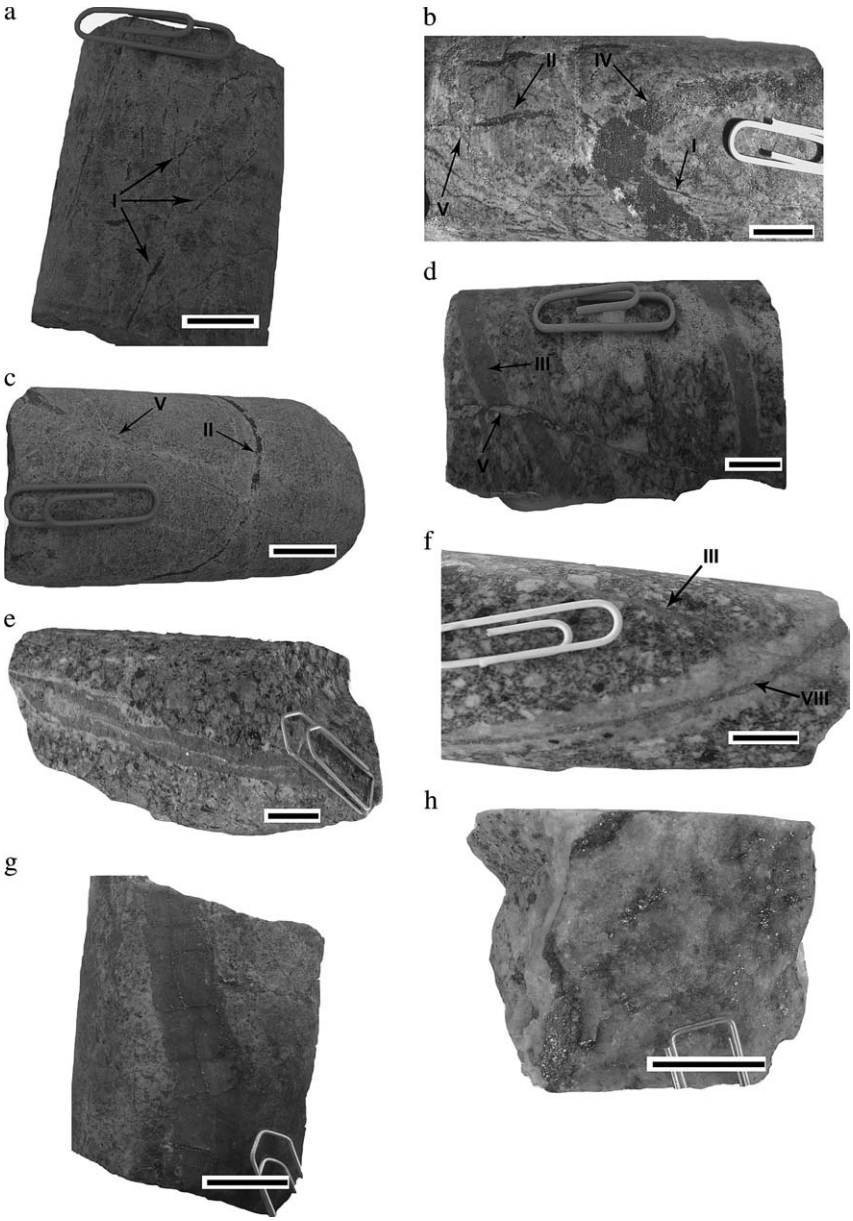

Fig. 6 Cross-cutting relationships of vein types at Miduk deposit. (a) Stockwork type I magnetite veinlets; (b) type I magnetite, type II quartz-magnetite, type IV quartz-magnetite-chalcopyrite and type V chalcopyrite-anhydrite veins in the P2 porphyry. Note that type IV cuts type I and II and type V cut types I, II and IV veins; (c) chalcopyrite vein (type V) cuts quartz-magnetite vein (type II) in the P1 porphyry; (d) barren quartz vein cut by chalcopyrite vein in the P2 porphyry. (e) Barren quartz veins with white center line of calcite, K-feldspar and sericite in the P2 porphyry; (f) pyrite vein (type VIII) with phyllic alteration halo in the P2 porphyry that cuts barren quartz vein (type III); (g) vein type VI with chalcopyrite–pyrite in the center line of the vein; (h) molybdenite vein (type VII) with quartz and minor chalcopyrite located in the margin of the veins. Molybdenite occurs as very fine anhedral to euhedral flakes. K-feldspar and minor sericite are the main alteration minerals in these veins (bar, 1 cm).

biotite represent the alteration minerals along these veins. These veins are associated with magnetite-rich potassic, potassic, potassic–phyllic and phyllic alteration zones and cut sharply the I and II vein types (Fig. 6b) and are present in the P1 and P2 porphyry.

7.5. Chalcopyrite–anhydrite veinlets and veins

These veins consist of chalcopyrite and anhydrite with a minor amount of quartz. The width of the veins ranges from <2 mm to 5 mm. In some of these, chalcopyrite is located in the central part of the veins with minor calcite, chlorite and sericite in the margin. Also, these veins cut plagioclase phenocrysts, and a K-feldspar alteration halo is formed around them. These veins are associated with potassic alteration zone and cut barren quartz (type III) veins (Fig. 6d), quartz–magnetite (type II) veins (Fig. 6c) and quartz-magnetite-chalcopyrite veins (type IV) (Fig. 6b).

7.6. Quartz-chalcopyrite-anhydrite-pyrite veins

These veins are thicker than the type V and mainly consist of quartz and chalcopyrite (Fig. 6g). Quartz grains

have a granular (mosaic) texture and their size increases from walls to the center of the veins. This may be due to reopening of the veins. In some of these veins coarse-grained quartz is located in the margin of veins and small quartz grains ar e located in the center. Chalcopyrite (5–250 μm) and pyrite (20–200 μm) are mainly located in the central line of veins and sometimes veinlets of pyrite and chalcopyrite cut these veins. Alteration halos around these veins contain K-feldspar-biotite (potassic alteration) or K-feldspar-sericite (potassic–phyllic alteration).

7.7. Quartz-molybdenite-anhydrite ± chalcopyrite ± magnetite veins

These veins are continuous, have straight walls and are narrow (<5 mm in width; Fig. 6h). Quartz grains have a granular texture and anhydrite grains are anhedral and larger than quartz grains. Magnetite and chalcopyrite are present in minor amount within potassic alteration zone.

7.8. Pyrite veinlets and veins

The thickness of these veins ranges from 1 to 30 mm. They occur in the deepest part of the deposit and are very narrow, continuous and cut plagioclase phenocrysts, have a sheeted structure and are associated with potassic alteration zone. In the upper part of the deposit these veins are thicker, continuous and consist of relatively coarse-grained pyrite, have intense fracturing and micro-brecciation and occur within the phyllic alteration zone. They cut sharply barren quartz veins and the quartz-chalcopyrite-pyrite-anhydrite veins.

7.9. Quartz–pyrite-anhydrite ± sericite veins

They are thick and continuous (1–5 cm) and consist relatively of coarse-grained pyrite, quartz, a minor amount of anhydrite and flakes of sericite. Quartz is present in the margin of the veins. Copper-bearing minerals are typically absent. A quartz–sericite alteration halo has developed around the veins. They are relatively scarce in the deeper levels of the deposit but probably represent the most abundant and widespread vein types in phyllic alteration zone at the Miduk deposit.

8. Re-Os geochronology

Re-Os age dating of molybdenite provides a robust chronometer for molybdenite mineralization (e.g. Stein *et al.*, 1997, 2001; Watanabe & Stein, 2000; Selby & Creaser, 2001). Molybdenite usually contains a high level of Re and no initial Os content. The Re-Os dating of molybdenite is important and robust to constrain the direct age determination of mineralization. Recently, with the development of precise Re-Os dating techniques, the determination of the different magmatic events and duration of hydrothermal activity is possible.

8.1. Previous geochronologic work

Previous U/Pb zircon, Rb-Sr and $^{40}Ar/^{39}Ar$ age data for magmatic and hydrothermal zones in the Miduk deposit are summarized in Table 4.

McInnes *et al.* (2005) demonstrated U/Pb zircon dating on the Miduk deposit and the Abdar (Masahim) prospect, hosted within partly eroded caldera of the Masahim stratovolcano. According to McInnes *et al.* (2005) the U/Pb zircon of this deposit is 12.5 ± 0.1 Ma and 7.5 ± 0.1 Ma, respectively. The mineral–whole rock Rb-Sr age of the Miduk porphyry is 12.4 ± 0.2 Ma (Hassanzadeh, 1993), but Hassanzadeh (1993) notes that the Rb-Sr age data do not seem to be reliable due to Rb addition and Sr depletion during potassic or magnetite-rich (A type veins) alteration. Hassanzadeh (1993) also reported the age of potassic and phyllic alteration events using $^{40}Ar/^{39}Ar$ dating. The age of potassic alteration zone, using biotite and K-feldspar, is 11.3 ± 0.5 Ma and 11.2 ± 0.4 Ma, respectively. He also determined a $^{40}Ar/^{39}Ar$ isochron age of 10.8 ± 0.4 Ma for sericite in the phyllic alteration zone.

8.2. Re-Os molybdenite age

The results of Re-Os dating of molybdenite are reported in Table 5. Two samples of disseminated and vein-type molybdenite in potassic alteration zone were collected from the deep part of the Miduk deposit, and they are affected by K-feldspar-sericite and minor secondary biotite alteration minerals. The molybdenite grains occur as flakes and are disseminated within anhydrite. Molybdenite from the Miduk deposit is hosted by the P2 porphyry and yield Middle Miocene ages. As shown in Table 4, the age determined for vein-type and disseminated molybdenite is 12.36 ± 0.07 Ma and 12.10 ± 0.07 Ma (2σ error), respectively. These ages are slightly younger than that given for U/Pb zircon dating (12.5 ± 0.1 Ma) reported by McInnes *et al.* (2005). According to McInnes *et al.* (2005), the P2 porphyry stock is emplaced at 12.5 ± 0.1 Ma. A U/Pb zircon age for P2 porphyry stock (12.5 ± 0.1 Ma) demonstrates that molybdenite mineralization is essentially contemporaneous with the emplacement of

Table 4 Previous radiometric ages for the Miduk porphyry copper deposit

Material analyzed	Alteration	Analytical method	Age (2σ) Ma	References
Zircon	P2 porphyry	U/Pb	12.5 ± 0.1	McInnes *et al.* (2005)
Mineral-whole rock	Potassic	Rb-Sr	12.4 ± 0.2	Hassanzadeh (1993)
Biotite	Potassic	$^{40}Ar/^{39}Ar$	11.3 ± 0.5	Hassanzadeh (1993)
K-feldspar	Potassic	$^{40}Ar/^{39}Ar$	11.2 ± 0.4	Hassanzadeh (1993)
Sericite	Phyllic	$^{40}Ar/^{39}Ar$	10.8 ± 0.4	Hassanzadeh (1993)

Table 5 Re-Os isotope data for molybdenite at the Miduk porphyry copper deposit

Minerals	Occurrence	Wall-rock alteration halo	^{187}Os (ppb)	Re (ppm)	Age (Ma)
Molybdenite	Molybdenite ± quartz ± chalcopyrite ± anhydrite	K-feldspar, minor biotite and sericite	158.23	1229.9	12.36 ± 0.07
Molybdenite	Fine molybdenite flakes disseminated with anhydrite	K-feldspar, anhydrite and minor biotite	153.65	1221.84	12.10 ± 0.07

the P2 porphyry. Comparison of these ages is given in Figure 7.

Recently many authors have used Re-Os dating of molybdenite for linking mineralization to magmatic activity (Selby *et al.*, 2002; Selby *et al.*, 2003; Hulbert & Hamilton, 2005). This connection is established by comparing the Re-Os dating of molybdenite and U/Pb zircon dating. The relationship between mineralization and magmatic activity using Re-Os and U/Pb zircon dating has been reported for many deposits: Grasberg, Indonesia (Mathur *et al.*, 2000; McInnes *et al.*, 2005), Chuquicamata (Ruiz & Mathur, 1999; Ballard *et al.*, 2001), Tintina Gold Belt, Alaska (Selby *et al.*, 2002), Thompson Nickel Belt (Hulbert & Hamilton, 2005), Tombstone Gold Belt, Yukon, Canada (Selby *et al.*, 2003) and the Endako porphyry molybdenum deposit (Selby & Creaser, 2001).

9. Magmatism and porphyry copper mineralization in the Miduk area

Magmatic events in the Central Iranian volcano-plutonic belt are closely related to subduction of Neotethys oceanic lithosphere within Central Iranian

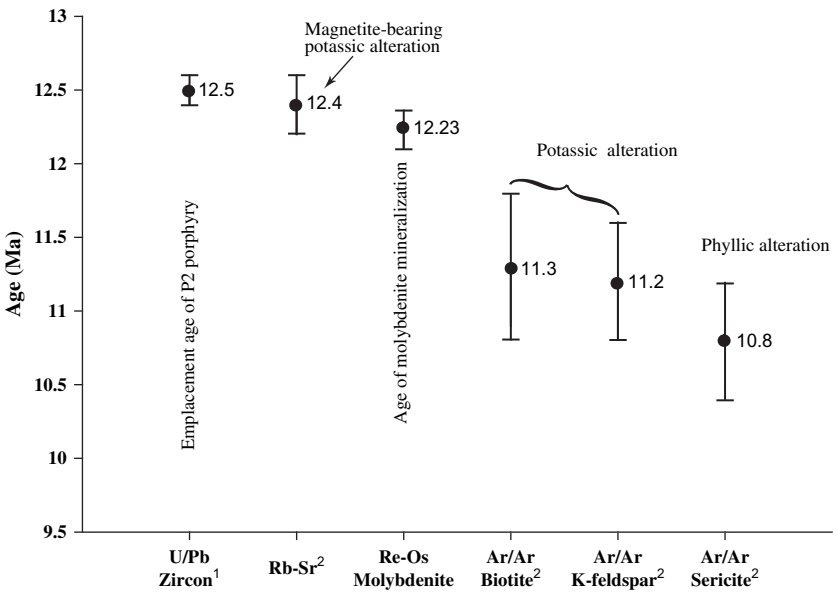

Fig. 7 Comparison of the previous geochronologic dating with Re-Os dating of molybdenite at Miduk deposit (Hassanzadeh, 1993; McInnes *et al.*, 2005).

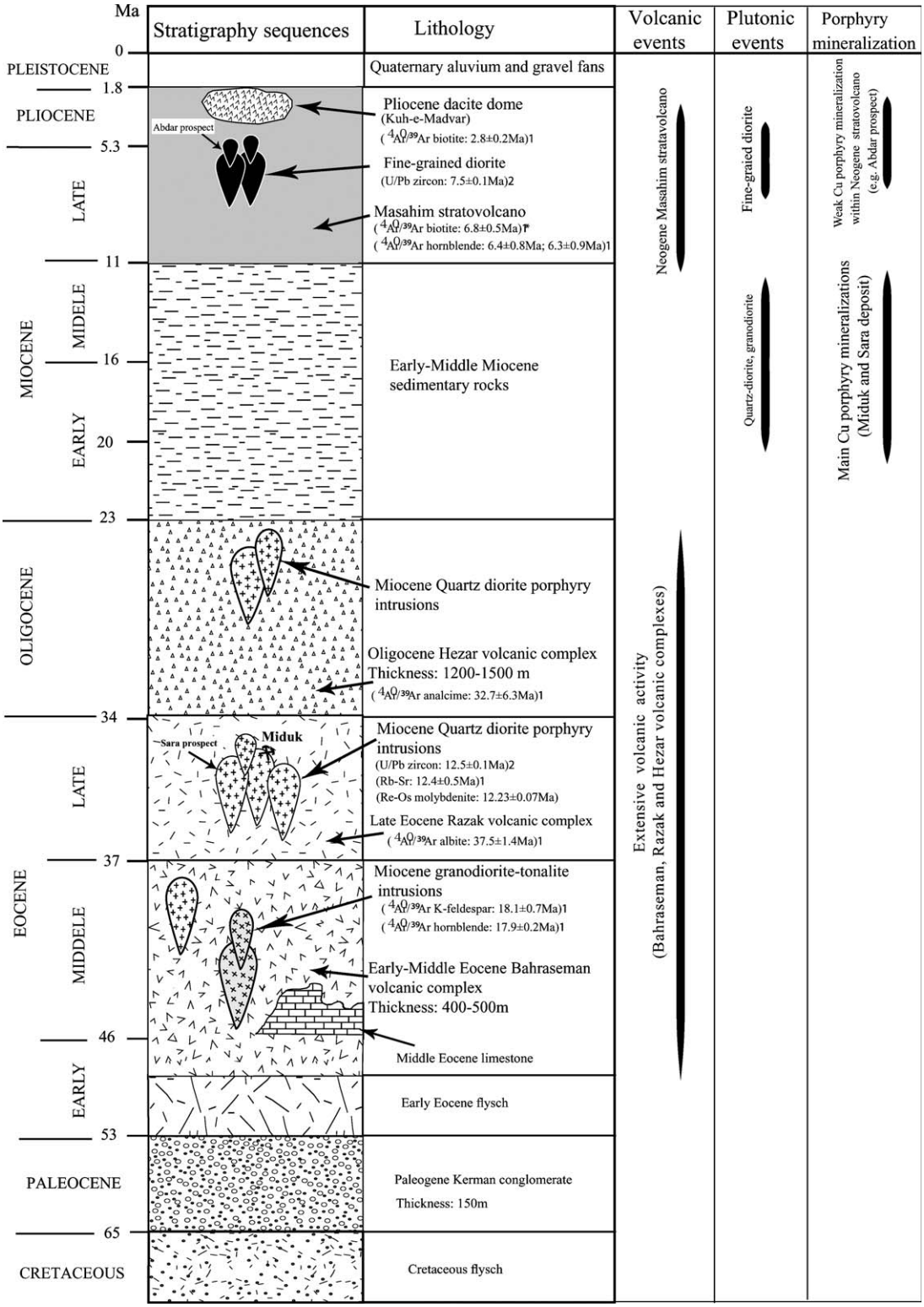

Fig. 8 Stratigraphy sequences, volcano-plutonic events and porphyry copper mineralization episodes in the Miduk area. (*Age of the lava flows on flanks of Masahim stratavolcano, Hassanzadeh, 1993; McInnes *et al.*, 2005.)

Table 6 Comparison of the Miduk porphyry copper deposit with other porphyry deposits†

	Miduk	Northern Chile	Philippines
Tectonic setting	Continental arc	Continental arc	Oceanic arc
Intrusion rocks	Diorite, quartz diorite, granodiorite?	Tonalite-granodiorite-monzogranite	Diorite-quartz diorite
Volcanic rocks	Andesite-basalt	Andesite, dacite	Andesite
K silicate alteration	Ore–related, abundant K feldspar	Ore–related, abundant K feldspar	Ore–related, minor K feldspar
Sericite alteration	Widespread	Widespread	Very restricted
Quartz stockwork	Abundant	Abundant	Abundant
Hypogene Fe oxide (M type veins)	Present minor in some ore zones	Present (but minor) in some ore zones	Abundant in ore zones
Mo/Au	853	1195‡	330‡
Deposit size	Medium: 170 Mt	Large: 500 Mt	Medium: 50–250 Mt
Supergene enrichment	Well developed	Well developed	Absent

†Data from northern Chile and Philippines from Vila & Sillitoe (1991).
‡Modified after Singer *et al.* (2005).

Table 7 Comparison of the Miduk, Sarcheshmeh and Sungun porphyry copper deposits in Iranian copper belt

	Miduk	Sarcheshmeh	Sungun
Tectonic setting	Continental	Continental	Continental
Volcanic rocks	Andesite-basalt	Andesite†	Dacite, trachy-andesite‡
Intrusive rocks	Diorite, quartz- diorite, granodiorite?	Granodiorite-quartz monzonite†	Diorite- granodiorite, quartz monzonite§
Emplacement depth (km)	2.51¶	4.75¶	2§
Emplacement Age (Ma)	12.5 ± 0.1¶	13.6 ± 0.1¶	Miocene§
Alteration types	Magnetite–rich potassic, potassic, Potassic–phyllic, propylitic, phyllic, argillic	Potassic, propylitic, phyllic ± argillic†	Potassic, propylitic, albitic, potassic-phyllic, phyllic, argillic §,††
M-type veins	Present	Absent	Absent
Anhydrite	Widespread	Abundant	Abundant
Tonnage (Mt)	170¶	1200†	600‡
Cu (%)	0.82	0.64†	0.76§
Au (ppb)	82	60‡‡	17§§
Ag (ppm)	1.80	1.14‡‡	2.2§§
Mo (%)	0.007	0.03¶¶	0.01§
Metallic type	Cu-Au-Ag	Cu-Mo-Au-Ag‡‡	Cu –Mo-Ag§§
Supergene enrichment	Well developed	Well developed	Restricted§§

†Waterman and Hamilton (1975).
‡ Hezarkhani and Williams-Jones (1998).
¶McInnes *et al.* (2005).
††Calagari (2004).
‡‡ Shafiei *et al.* (2000).
§§ Tabatabaei (2002).
¶¶Shahabpour (2000).

plateau. It is believed that the opening of Neotethys started in the Permian and that the collision of the Arabian and Iranian plates occurred during the end of the Miocene (Forster, 1978; Berberian & King, 1981; Berberian *et al.*, 1982). The main volcanic activity began in the Lower Eocene with the Bahraseman complex, Middle–Upper Eocene Razak complex and Oligocene Hezar complex. These complexes comprise the main volcanic activity in the area, with thickness approximately 11–16 km in the Kerman belt. The lithologic sequences, volcanic and plutonic events and porphyry-type mineralization are shown in Figure 8. The plutonic phases were formed in two stages in the Middle Miocene, with quartz–diorite, granodiorite and Late Miocene diorite intrusions within the caldera of the Masahim stratovolcano. The Miduk porphyry copper deposit ($^{40}Ar/^{39}Ar$, 11.3 ± 0.5 Ma, Hassanzadeh, 1993; zircon U/Pb, 12.5 ± 0.1 Ma, McInnes *et al.*, 2005; Re-Os molybdenite, 12.23 ± 0.07 Ma, present study) and the Sara porphyry copper prospect ($^{40}Ar/^{39}Ar$, 13.3 ± 1.1 Ma, Hassanzadeh, 1993) were formed by Middle Miocene intrusions in the Miduk area. Also, the Sar Cheshmeh porphyry copper deposit was formed in the Middle Miocene (K-Ar, 12.5 ± 0.5 Ma and Rb-Sr, 12.2 ± 1.2 Ma, Shahabpour, 1982; zircon U/Pb, 13.6 ± 0.1 Ma, McInnes *et al.*, 2005). Abdar porphyry copper prospect is formed along with Late Miocene diorite intrusion (zircon U/Pb, 7.5 ± 0.1 Ma, McInnes *et al.*, 2005) within the partly eroded caldera of the Masahim stratovolcano. The latest intrusive activity in the Miduk area is related to subvolcanic dacitic domes that formed in the Pliocene ($^{40}Ar/^{39}Ar$, 2.8 ± 0.2 Ma, Hassanzadeh, 1993).

10. Comparison with other porphyry copper deposits in the world and Iran

The data presented in Table 6 demonstrate that the Miduk porphyry copper deposit, aside from tonnage and composition of the intrusive phase, is likely similar to porphyry copper deposits of continental arc settings such as northern Chile. This is indicated by the presence of the large andesite–dacite Masahim stratovolcano in the Miduk area and the thick volcanic sequences (11–16 km) of Paleogene (Bahraseman, Razak and Hezar volcanic complexes) in the Kerman volcano-plutonic belt. Alteration and mineralization zones in the Miduk deposit are similar to typical continental arc porphyry copper deposits described by Lowell and Guilbert (1970). Magnetite-rich potassic zone that presents in the Miduk deposit is similar to the island-arc copper deposit, British Columbia (Arancibia & Clark, 1996) and the Bajo de La Alumbrera deposit, Argentina (Ulrich & Henrich, 2001).

The vein mineralization in the Miduk deposit includes all of the vein types described by many workers in continental arc porphyry copper deposits. The A, B, C and D veins previously described by Gustafson and Hunt (1975) at the El Salvador deposit and Dilles and Einaudi (1992), are also present in the Miduk deposit. Also, the M type veins described by Clark (1993), Clark and Arancibia (1995), Arancibia and Clark (1996) and Ulrich and Henrich (2001) occur typically at the Miduk deposit.

Table 7 lists the comparison of the Miduk deposit with the Sar Cheshmeh and the Sungun porphyry copper deposits in the Central Iranian porphyry copper belt. Except for some similarities (tectonic setting, volcanic rocks, ages and alteration types), there are some differences, as follows.

Emplacement depth of the Miduk deposit was determined by McInnes *et al.* (2005) (2.51 km) to be deeper than the Sungun deposit (2 km, Hezarkhani & Williams-Jones, 1998; determined by fluid inclusion study) and shallower than the Sar Cheshmeh deposit (4.75 km, McInnes *et al.*, 2005). In contrast, the depth of emplacement of these deposits increases from north (Sungun deposit) to south (Miduk and Sar Cheshmeh deposit) in the Central Iranian copper belt (Fig. 1). Magnetite-rich potassic, M-type mineralization is present only in the Miduk deposit, and anhydrite mineralization is well developed. The Cu and Au values in the Miduk deposit are higher than in the Sar Cheshmeh and the Sungun deposits.

11. Conclusions

The Miduk porphyry copper deposit is located in the Central Iranian volcano-plutonic belt and is associated with calc-alkaline intrusive rocks of Miocene age that intruded the Eocene Razak volcanic complex. The main mineralization occurred in P2 porphyry (Miduk porphyry) and the volcanic wall rocks contain <10% of mineralization.

The magnetite-rich zone occurred as veinlets (M1 type), vein (M2 type) and dissemination and is related to an early stage of mineralization. It is observed in the deepest part of this deposit associated with K-feldspar, quartz, and minor amounts of biotite and chlorite. The main stage of mineralization contains chalcopyrite occurrence with quartz, magnetite and anhydrite as veinlets; and veins in potassic alteration zone with abundant K-feldspar and secondary biotites.

The Re-Os molybdenite dates indicate that the sulfide mineralization occurred at 12.23 ± 0.07 Ma. These

dates are significantly similar to zircon U/Pb ages and demonstrate that molybdenite mineralization was contemporaneous with emplacement of P2 porphyry. The Re-Os age of the Miduk deposit indicates that the main stage of magmatism and porphyry copper formation occurred in the Middle Miocene (Miduk and Sar Cheshmeh deposits) in the Kerman belt.

On comparing the Miduk deposit with several porphyry copper ores from around the world, along with mineralogy, alteration halos and geochemistry, it is concluded that the Miduk porphyry copper deposit is very similar to those of continental arc settings.

Acknowledgments

This study is a part of the first author's PhD thesis carried out under the supervision of the second author at Shahid Bahonar University of Kerman, Iran. The authors would like to thank the National Iranian Copper Industries Company (NICICO) for providing access to Miduk, and permission to publish the data and for supplying the important unpublished databases. Thanks to Mr Ramezami and Mrs Abaslu and Mr Shafiei for field work and sampling. The authors appreciate the kind cooperation of Fernando Barra and the University of Arizona for assistance with the Re-Os analyses. This paper benefited from constructive reviews by Dr Akira Imai, Dr Arifudin Idrus and one anonymous Resource Geology referee. This work was supported by grants from NICICO and Shahid Bahonar University of Kerman.

References

Aftabi, A. and Atapour, H. (2000) Regional aspects of shoshonitic volcanism in Iran. Episodes, 23, 119–125.

Alavi, M. (1994) Tectonics of the Zagros orogenic belt of Iran: New data and interpretations. Tectonophys., 229, 211–238.

Arancibia, O. N. and Clark, A. H. (1996) Early magnetite-plagioclase alteration-mineralization in the Island Copper porphyry copper-gold-molybdenum deposit, British Columbia. Econ. Geol., 91, 402–458.

Ballard, J. R., Palin, J. M., Williams, I. S., Campbell, I. H. and Faunes, A. (2001) Two ages of porphyry intrusion resolved for the super-giant Chuquicamata copper deposit of northern Chile by ELA-ICP-MS and SHRIMP. Geology, 29, 383–386.

Beane, R. E. and Bodnar, R. J. (1995) Hydrothermal fluids and hydrothermal alteration in porphyry copper deposits. In Pierce, F. W. and Bohm, J. G. (eds.) Porphyry copper deposits of the American Cordillera. Arizona Geological Society Digest 20, Tucson, AZ, 83–93.

Berberian, M. and King, G. C. P. (1981) Towards a paleogeography and tectonic evolution of Iran. Can. J. Earth Sci., 18, 210–265.

Berberian, F., Muir, I. D., Pankhurst, R. J. and Berberian, M. (1982) Late cretaceous and early Miocene Andean-type plutonic activity in northern Makran and Central Iran. J. Geol. Soc. (London), 139, 605–614.

Calagari, A. A. (2004) Fluid inclusion studies in quartz veinlets in the porphyry copper deposit at Sungun, East-Azarbaijan, Iran. J. Asian Earth Sci., 23, 179–189.

Clark, A. H. (1993) Are outsize porphyry copper deposits either anatomically or environmentally distinctive? Soc. Econ. Geol. Special Publ. 2, 213–283.

Clark, A. H. and Arancibia, O. (1995) Occurrence, paragenesis and implications of magnetite-rich alteration-mineralization in calc-alkaline porphyry copper deposits. *In* Clark, A. H. (ed.) Giant ore deposits: II. Controls on the scale of orogenic magmatic-hydrothermal mineralization. Department of Geological Sciences, Queen's University, Kingston, ON, 583–640.

Creaser, R. A., Papanastassiou, D. A. and Wasserburg, G. J. (1991) Negative thermal ion mass spectrometer of Os, Re and Ir. Geochim. Cosmochim. Acta, 55, 397–401.

Dilles, J. H. and Einaudi, M. T. (1992) Wall-rock alteration and hydrothermal flow paths about the Ann-Mason porphyry copper deposit, Nevada: 6 km vertical reconstruction. Econ. Geol., 87, 1963–2001.

Dimitrijevic, M. (1973) Geology of Kerman region. (Iran Geological Survey Report No. Yu/52.) Institute for Geological and Mining Exploration and Institution of Nuclear and Other Mineral Raw Materials, Beograd-Yugoslavia, 334p.

Forster, H. (1978) Mesozoic–Cenozoic metallogenesis in Iran. J. Geol. Soc. (London), 135, 443–455.

Frei, R., Nagler, T., Schonberg, R. and Kramers, J. (1998) Re-Os, Sm-Nd, U-Pb and stepwise lead leaching isotope systematics in shear zone hosted gold mineralization: Genetic tracing and age constraints of crustal hydrothermal activity. Geochim. Cosmochim. Acta, 62, 1925–1936.

Gustafson, L. B. and Hunt, J. P. (1975) The porphyry copper deposit at El Salvador, Chile. Econ. Geol., 70, 857–912.

Hassanzadeh, J. (1993) Metallogenic and tectono-magmatic events in SE sector of the Cenozoic active continental margin of Central Iran (Shahr-Babak, Kerman Province) (PhD Thesis). University of California, Los Angeles, 201p.

Hezarkhani, A. and Williams-Jones, A. E. (1998) Controls of alteration and mineralization in the Sungun porphyry copper deposit, Iran: Evidence from fluid inclusions and stable isotopes. Econ. Geol., 93, 651–670.

Hulbert, L. J. and Hamilton, M. A. (2005) U-Pb Zircon and Re-Os isotope geochronology of mineralized ultramafic intrusions and associated nickel ores from the Thompson Nickel Belt, Manitoba, Canada. Econ. Geol., 100, 29–41.

Hutchinson, C. S. (1974) Laboratory handbook of petrographic techniques. John Wiley & Sons, New York, 527p.

Institute for Geological and Mining Exploration and Institution of Nuclear and Other Mineral Raw Materials (1973) Exploration for ore deposits in Kerman Region. (Iran Geological Survey Report No. Yu/53.) Iran Geological Survey, Beograd-Yugoslavia, 247p.

Lowell, J. D. and Guilbert, J. M. (1970) Lateral and vertical alteration zoning in porphyry ore deposits. Econ. Geol., 65, 373–408.

Mathur, R. (2000) Re-Os isotopes of base metal porphyry deposits (PhD Thesis). University of Arizona, Tucson, 153p.

Mathur, R., Ruiz, J., Titley, S., Gibbins, S. and Margotomo, W. (2000) Different crustal sources for Au-rich and Au-poor ores

of the Grasberg Cu-Au porphyry deposit. Earth Planet. Sci. Lett., 183, 7–14.

McCandless, T. E. and Ruiz, J. (1993) Rhenium-osmium evidence for regionally-timed mineralization events in southwestern North America. Science, 261, 1282–1286.

McInnes, B. I. A, Evans, N. J., Fu, F. Q. and Garwin, S. (2005) Application of thermochronology to hydrothermal ore deposits. Rev. Mineral. Geochem., 58, 467–498.

Mohajjel, M., Fergussen, C. L. and Sahandi, M. R. (2003) Cretaceous-Tertiary convergence and continental collision, Sanandaj-Sirjan zone, Western Iran. J. Asian Earth Sci., 21, 397–412.

Outomec, (1992) Techno-economic feasibility study and relevant backing technical studies of Miduk Copper Project. Outokumpu, Finland, 171p.

Ruiz, J. and Mathur, R. (1999) Metallogenesis in continental margins: Re-Os evidence from porphyry copper deposits in Chile. Rev. Econ. Geol., 12, 59–72.

Saric, A., Djordjevic, M. and Dimitrijevic, M. N. (1971) Geological map of Shahr-Babak, Scale 1/100000. Geological Survey of Iran, Tehran, Iran.

Selby, D. and Creaser, R. A (2001) Re-Os geochronology and systematics in molybdenite from the Endako porphyry molybdenum deposit, British Columbia, Canada. Econ. Geol., 96, 197–204.

Selby, D., Creaser, R. A., Hart, C. J. R., Cameron, S., Rombach, C. S., Thompson, J. F. H., Smith, M. T., Bakke, A. A. and Goldfarb, R. J. (2002) Absolute timing of sulfide and gold mineralization: A comparison of Re-Os molybdenite and Ar-Ar mica methods from the Tintina Gold Belt, Alaska. Geology, 30, 791–794.

Selby, D., Creaser, R. A., Heaman, L. M. and Hart, C. J. R. (2003) Re-Os and U-Pb geochronology of the Clear Creek, Dublin Gulch, and Mactung deposits, Tombstone Gold Belt, Yukon, Canada: Absolute timing relationships between plutonism and mineralization. Can. J. Earth Sci., 40, 1839–1852.

Shafiei, B., Shahabpour, J. and Sadloo, M. (2000) Geochemical characteristics, nature, and genesis of hypogene gold and silver in the Sar Cheshmeh porphyry copper deposit, Kerman. Geosciences, 8, 34–49 (in Persian with English abstract).

Shahabpour, J. (1982) Aspect of alteration and mineralization at the Sar Cheshmeh Copper-molybdenum deposit, Kerman, Iran (PhD Thesis). Leeds University, Leeds, 342p.

Shahabpour, J. (2000) Behaviour of Cu and Mo in the Sar Cheshmeh porphyry Cu deposit, Kerman, Iran. CIM Bull., 93, 44–51.

Shirey, S. and Walker, R. (1995) Carius tube digestion for low-blank rhenium-osmium analysis. Anal. Chem., 67, 2136–2141.

Singer, D. A., Berger, V. I. and Moring, B. C. (2005) Porphyry copper deposit in the world: Database, map and grade and tonnage models. (USGS Open-file Report 2005-1060.) US Geological Survey, Denver, 9p.

Smoliar, M. I., Walker, R. J. and Morgan, J. W. (1996) Re-Os ages of group IIA, IIIA, IVA and IVB iron meteorites. Science, 271, 1099–1102.

Stein, H. J., Markey, R. J., Morgan, J. W., Du, A. and Sun, Y. (1997) Highly precise and accurate Re-Os age for molybdenite from the East Qinling molybdenite belt, Shaanxi Province, China. Econ. Geol., 92, 827–835.

Stein, H. J., Markey, R. J., Morgan, J. W., Hannah, J. L. and Schersten, A. (2001) The remarkable Re-Os chronometer in molybdenite: How and why it works. Terra Nova, 13, 479–781.

Tabatabaei, D. (2002) Geochemical investigation on the exploration significance of the lithogeochemical haloes at the Sungun porphyry (Cu-Mo)–skarn (Cu-Ag-Au), Ahar, Azerbaijan (MSc Thesis). Shahid Bahonar University of Kerman, Kerman, 376p.

Ulrich, T. and Henrich, C. (2001) Geology and alteration geochemistry of the porphyry Cu-Au deposit at Bajo de la Alumbrera, Argentina. Econ. Geol., 96, 1719–1742.

Vila, T. and Sillitoe, R. H. (1991) Gold-rich porphyry systems in the Maricunga belt, northern Chile. Econ. Geol., 86, 1238–1260.

Watanabe, Y. and Stein, H. J. (2000) Re-Os ages for the Erdenet and Tsagaan Suvarga porphyry Cu-Mo deposits, Mongolia, and tectonic implications. Econ. Geol., 95, 1537–1542.

Waterman, G. C. and Hamilton, R. L. (1975) The Sar Cheshmeh porphyry copper deposit. Econ. Geol., 70, 568–576.